Materials Science Forum Vols. 22-24 (1987) pp. 269-282

PHASE TRANSITIONS OF A PREDOMINANTLY ICOSAHEDRAL MATERIAL

Steven M. Anlage
Applied Physics
California Institute of Technology
Pasadena, California 91125 USA

ABSTRACT

We examine the consequences of short-range icosahedral order in metastable metallic alloys. There is evidence, both direct and indirect, for the existence of atomic clustering with icosahedral symmetry in supercooled liquid metals, metastable metallic alloys, and large-unit-cell intermetallic compounds. It is observed that a variety of metallic alloys can exhibit a long-range ordered structure with icosahedral point group symmetry upon rapid quenching from the liquid.

We have developed a theory to explain qualitatively how a phase with enhanced short-range icosahedral order forms from the melt. A model material is proposed which is endowed with short-range icosahedral order broken up by defect structures. The thermodynamics of this model are described by a Ginzburg-Landau theory. The model displays a first-order phase transition from a high-temperature heavily defected phase to a low-temperature phase with enhanced short-range icosahedral order.

1. Evidence of Icosahedral Ordering in Metals

1.1 Historical Overview

Until quite recently, little serious consideration has been given to the possibility of atomic clustering with icosahedral symmetry in condensed matter. The symmetry group of the icosahedron includes 12 five-fold rotation axes passing through its opposite vertices. In classical crystallography, which assumes that all structures can be built up by a periodic tesselation of space with a single unit cell, global five-fold symmetry axes are impossible [1,2,3]. This fact is related to the observation that regular tetrahedra and icosahedra cannot be used to tesselate space without overlapping or leaving gaps [4]. For this reason the mainstream of condensed matter research has flowed away from consideration of 5-fold and icosahedral symmetries in metallic systems. Despite the belief that icosahedral symmetry was not possible in metallic crystals, a number of workers maintained that small clusters of atoms with this symmetry could be found in liquid metals, intermetallic compounds and metallic glasses.

1.2 Evidence of Icosahedral Ordering in Liquid Metals

Metallic bonding favors configurations in which the number of nearest neighbors around a given atom is maximized [5]. The bonding properties of metallic atoms are nearly isotropic, so the atom can be profitably modeled as a sphere of some appropriate radius. The maximum number of equal size spheres that can be in contact with a given sphere is twelve [6]. Locally, this can be achieved in three different ways, face-centered cubic (FCC) packing, hexagonal close-packing (HCP) and an icosahedral cluster. Frank has noted that an icosahedral grouping of thirteen atoms interacting through a Lennard-Jones potential has a binding energy 8.4% less than similarly sized clusters of face-centered cubic or hexagonal close-packing [6].

Hoare et al. [7,8] have calculated the minimum energy structures of finite clusters of atoms interacting by central two-body Lennard-Jones interactions. They find that such clusters tend to grow in one of three modes; tetrahedral, pentagonal or icosahedral, rather than as FCC or HCP clusters. None of these minimum energy growth modes can be continued indefinitely to fill all space; they suffer from 'self-limiting growth' [8]. These clusters are referred to as 'anti-crystalline.' This topological frustration (i.e. the inability to fill space with a minimum energy configuration) gives rise to interesting effects when materials are constrained to adopt such growth modes in favor of crystalline growth. For instance, Tammann [see ref. 8] has proposed that the rise in viscosity accompanying the glass transition in a supercooled liquid is due to the growth and mutual impingement of anti-crystalline units in the liquid.

A number of investigators have observed a variety of pre-freezing phenomena in liquid metal systems. Turnbull [9] and Perepezko [10] have supercooled elemental liquid metals (by eliminating heterogeneous nucleation sites) to 30-40% of the absolute melting temperature before crystallization begins by homogeneous nucleation. This deep excursion into the metastable regime implies the existence of relatively stable structures in the supercooled liquid. With these observations in mind, Frank [6] proposed that icosahedral clustering in the supercooled liquid metal is responsible for the deep supercooling. The icosahedral cluster is a low energy structure; its topological short-range order is also somewhat different from that of FCC or HCP crystals. The atomic rearrangements required to transform the cluster into one of the common crystal packings are energetically costly and can only be overcome when they are done on long length scales. This requires a substantial structural fluctuation which is only likely to occur at a certain degree of supercooling (in the absence of a seed crystal). In other words, icosahedral clustering presents a nucleation barrier for crystallization of the liquid metal, thus explaining the observed supercooling properties.

1.3 Evidence of Icosahedral Ordering in Intermetallic Compounds

It is known that many intermetallic crystal structures have large unit cells with many atoms in the basis [11]. To simplify the structural refinement of these crystals, Samson has developed a technique to represent the crystal basis as a packing of coordination polyhedra [12]. One of the most common coordination polyhedra in intermetallic compounds has coordination 12 and is isomorphic to the icosahedron. Samson has identified several other common coordination polyhedra involving higher coordinations [12]. These include the Friauf polyhedra (coordination number (CN) 16), the μ – phase polyhedra (CN 15), the hexagonal prism and anti-prism (CN 14) and a few other irregular polyhedra.

Consider the following represntative large unit cell crystal structures which have been reported in the literature. The $Al_{12}Mo$ crystal structure [13] consists of a molybdenum atom at each body centered cubic lattice site surrounded by an icosahedral cluster of

12 aluminum atoms. An example of more extensive icosahedral clustering is the crystal structure of $Mg_{32}(Zn,Al)_{49}$ [14]. This crystal also has a body-centered cubic lattice with an atom on each lattice site. Surrounding that atom are shells of atoms which sit on the vertices of an icosahedron, a larger dodecahedron, a still larger icosahedron, and a final shell of atoms making up a truncated icosahedron with tetrahedral symmetry. It is interesting to note that the icosahedral phase is found in samples of rapidly solidified liquids with composition $Al_{12}Mo$ and $Mg_{32}(Zn,Al)_{49}$.

Examination of these and many other intermetallic compounds [11,12] lead one to the following conclusion. When atoms are in the basis of a large unit cell metallic crystal (hence relatively free of crystallographic constraints) they may cluster into units having non-crystallographic symmetry. The fact that these non-crystallographic groupings are predominant in the basis is a reflection of their stability and simplicity. This is yet another reason why icosahedral clustering must be taken seriously in any theory of the structure of metals.

1.4 Evidence of Icosahedral Ordering in Metallic Glasses

Bernal's [15] dense random packing of hard spheres was an early attempt to model the structure of a metallic glass. This model includes the qualitative features of a metallic glass with an isotropic, purely repulsive pair interaction. Since the model has no attractive term in the interaction potential, one does not expect to find an abundance of the low energy tetrahedral and icosahedral clusters in the structure. To go beyond these simplistic hard sphere packing models a number of researchers have modeled the glassy state with more sophisticated interaction potentials by means of computer simulated quenches of Lennard-Jones potential liquids.

To extract more information from these computer simulations of Lennard-Jones liquids, Steinhardt, Nelson and Ronchetti [16,17] defined a set of bond orientational order parameters. Steinhardt et al. evaluated these order parameters for a super-cooled Lennard-Jones liquid and noted a dramatic increase in the value of the icosahedral bond orientational order parameter and a much more modest increase in that for cubic orientational order. The observed increase in the icosahedral bond-orientational order parameter started a flurry of activity in the theory of metallic glasses.

Nelson [18], building on the ideas of Kléman [19] and Sadoc [20], later proposed that supercooled liquid metals and metallic glasses can be thought of as systems with defective icosahedral bond orientational order. This theory predicts a scattering structure factor in close agreement with those obtained experimentally on elemental amorphous thin metal films [21,22]. Like most other theories of disordered systems, Nelson's metallic glass model rests on the concept of frustration [23]. When 5 perfect tetrahedra are wrapped around a common edge, they will leave a deficit angle of about 7°. If we assign atoms to each of the vertices of this structure, it is clear that one of the atoms will not be in the potential energy minimum of all of its neighbors (in fact it has two equivalent choices). This local topological frustration is responsible for the global topological disordering in a material with atoms that prefer local tetrahedral coordination.

At the moment, computer simulations provide the only direct evidence for non-crystallographic clustering in metallic glasses. Despite this, the idea that a frustrated packing of icosahedral units is responsible for metallic glass formation has proven to be very fruitful. In summary, sections 1.2-1.4 have shown that when atoms in a metal are free from crystallographic constraints (e.g. in the basis of a large unit cell intermetallic compound, in a liquid metal, or in a metallic glass) they tend to group into low energy non-crystallographic clusters. This structural motif must be taken into consideration if one wants to understand the structure and dynamics of non-crystalline metals.

1.5 The Icosahedral Phase

Direct experimental evidence of the existence of long-range icosahedral order in condensed matter came with the discovery by Schechtman et al. [24] of the icosahedral phase. This phase is distinguished by the fact that it diffracts electrons with the point group symmetry of an icosahedron. This point group is unique in condensed matter, and because of its global five-fold symmetry it is inconsistent with the tenet of classical crystallography which states that a crystal is made up of a periodic tiling of a single packing unit.

There are several interesting problems that have not yet been solved concerning the icosahedral phase. First, the atomic structure of the icosahedral phase has yet to be determined. This has not been done because the techniques of traditional crystallography are of little value when dealing with quasiperiodic structures. A second set of interesting problems concerns a comparison of the physical properties of amorphous, icosahedral and crystalline materials at the same composition. For instance, one would like to know if any new collective phenomena (e.g. phonons, superconductivity, and magnetism) are associated with the unique point group symmetry and structure of the icosahedral phase. A third question of interest concerns how and why the icosahedral phase forms from the liquid, vapor, or solid states. Understanding the formation conditions will allow us to predict which alloys will display the icosahedral phase and give us some clues about their atomic structure and properties.

This paper is devoted primarily to the third question raised above. We shall consider the thermodynamics of a model material which is endowed with icosahedral short-range order. Since we have seen that icosahedral clustering is a structural motif in certain metals, it is of interest to see if that kind of ordering can be extended to a global scale.

2. The Predominantly Icosahedral Material

2.1 The Physical Picture

Since the icosahedral phase is normally formed upon rapid quenching of the liquid, it may nucleate on the icosahedral clusters present in the supercooled liquid. If this is the case, then icosahedral clustering is a necessary prerequisite for formation of the icosahedral phase. To examine the behavior of a supercooled liquid metal, we propose a model for a predominantly icosahedral material (PIM). To help visualize the theory, a schematic diagram of a PIM is shown in Figure 1. The PIM is characterized by regions in which the atoms cluster into units having short-range icosahedral symmetry These regions need not be thirteen atom icosahedra; several other shells of atoms with icosahedral symmetry are also possible. We shall define an icosahedral order parameter that has a large value in the vicinity of these icosahedral clusters. Since the icosahedral units cannot pack together to fill space, there must be some regions between them where there is little or no icosahedral order. Later we shall see that these regions are in fact linear features and will be called disclination lines, since they represent a rotational anomaly about the line. Thus a PIM can be succinctly described as regions of local icosahedral order broken up by defect line structures.

Using the icosahedral order parameter and the defects, we can construct a theory for the thermodynamics of a PIM in analogy with the Ginzburg-Landau (GL) theory of superconductivity. In the GL theory, one expands the energy of the system near the transition temperature in powers of a 'small' order parameter, and includes terms for the energy associated with any external fields which may be present.

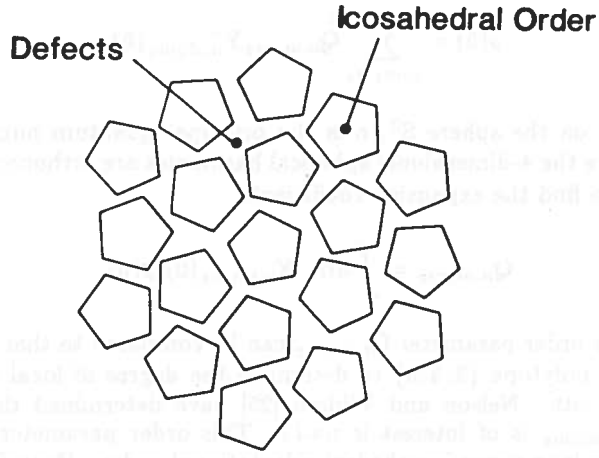

Figure 1. Schematic physical picture of the predominantly icosahedral material. Regions of high local icosahedral order are separated by linear defective structures.

2.2 Local Icosahedral Order Parameter

A local icosahedral bond orientational order parameter has been developed by Steinhardt and Nelson [17]. A somewhat more sophisticated local order parameter which takes into account both orientational and translational order was later developed by Nelson and Widom using the curved space description of amorphous materials [25]. As discussed in section 1.4, five perfect tetrahedra wrapped around a common edge will leave a deficit angle of about 7°. If space can be curved in such a way as to close up this deficit angle, then a tetrahedral tesselation of space may then be possible. Nelson used such a tesselation, originally proposed by Coxeter [26], known as polytope $\{3,3,5\}$. The Schläfli symbol [26] for a tetrahedron is $\{3,3\}$, denoting an object with three equilateral triangles that meet at a single point (in 3-dimensions). Polytope $\{3,3,5\}$ is a regular object with five perfect tetrahedra meeting along a common edge (in 4-dimensions).

Atoms can be assigned to the 120 vertices of polytope $\{3,3,5\}$ to produce a tetrahedral tesselation of curved 3-dimensional space. As discussed by Nelson and Widom [25] the ideal tesselation consists of a central atom surrounded by icosahedral, dodecahedral, larger icosahedral and icosidodecahedral shells. The environment of each vertex of polytope $\{3,3,5\}$ is equivalent and this local environment will represent what we expect to find in an ideal icosahedral material.

We now consider a quantitative measure for comparing a local configuration of atoms to the ideal structure of polytope $\{3,3,5\}$. Nelson and Widom [25] proposed that a given atom and its nearest neighbors be projected onto the surface of the 4-dimensional sphere S^3 based at the site of interest. This projection is then compared to a polytope $\{3,3,5\}$ of the same radius. A quantitative measure of how closely these two structures agree can

be made by comparing the expansion coefficients of the projected particle density $\rho(\hat{u})$ in terms of the 4-dimensional spherical harmonics Y_{n,m_1,m_2};

$$\rho(\hat{u}) = \sum_{n,m_1m_2} Q_{n,m_1m_2} Y^*_{n,m_1m_2}(\hat{u})$$

where $\hat{u}$ is a point on the sphere S^3, n is the principal quantum number and $-n/2 \leq m_1, m_2 \leq n/2$. Since the 4-dimensional spherical harmonics are orthonormal on the sphere S^3, we can invert to find the expansion coefficients;

$$Q_{n,m_1m_2} = \int d\Omega_{\hat{u}}\ Y_{n,m_1m_2}(\hat{u})\ \rho(\hat{u}).$$

The complex tensor order parameter Q_{n,m_1m_2} can be compared to that of the ideal icosahedral structure of polytope $\{3,3,5\}$ to determine the degree of local icosahedral ordering present at the site. Nelson and Widom [25] have determined that the first value of n for which Q_{n,m_1m_2} is of interest is n=12. This order parameter is capable of describing states with long-range icosahedral orientational order. Henceforth, we shall use Q_{12,m_1m_2} $(-6 \leq m_1, m_2 \leq 6)$ as our local icosahedral order parameter.

2.3 Disclination Lines

The experimentally observed crystalline structures which are most similar to an ideal icosahedral material are the intermetallic Frank-Kasper (FK) phases. The FK phases are simply defined as topologically close-packed intermetallic compounds with exclusively tetrahedral interstices between the atoms [27]. Of course many of these tetrahedra are distorted and irregular.

One can define a nearest-neighbor coordination polyhedron using the Voronoy method in real space. Because of the tetrahedral packing configurations, one finds that all faces of the nearest neighbor polyhedra will be triangular (although the triangles may be irregular), and that the polyhedron can be broken up into a collection of tetrahedra [27]. The central atom in an icosahedral cluster is a common point for twenty tetrahedra which make up the nearest neighbor coordination polyhedron. Each nearest neighbor bond is a common edge for a discrete number of tetrahedra. In the case of an icosahedral coordination, there are exactly five tetrahedra wrapped around every nearest neighbor bond.

Frank and Kasper identified four different kinds of coordination polyhedra in the FK phases; coordination number 12 (CN12), CN14, CN15 and CN16 [28,29]. In all of these coordination polyhedra there are only two kinds of nearest neighbor bonds; those surrounded by either five or six tetrahedra. Some metastable structures also involve nearest neighbor bonds surrounded by only four tetrahedra. These three types of nearest neighbor bonds are illustrated in Figure 2. Bonds surrounded by four or six tetrahedra are not found in icosahedral environments and are in the minority in the FK structures. These 'anomolous' bonds are referred to as disclinations since they represent a rotational anomaly in the structure (i.e. a deviation from five in the number of tetrahedra around the bond). Since one tetrahedron is either present or missing along these bonds, they are referred to as $\mp 72°$ disclination lines (with 72° being the dihedral angle of a regular tetrahedron). All of the nearest neighbor bonds of the central atom in an icosahedral cluster are surrounded by five tetrahedra, so that a disclination line connects two atoms which are not in icosahedral symmetry sites. It can be shown that these lines form a continuous network which

permeates the solid [18]. Disclination lines provide a shorthand notation for describing the structure of topologically close-packed metals.

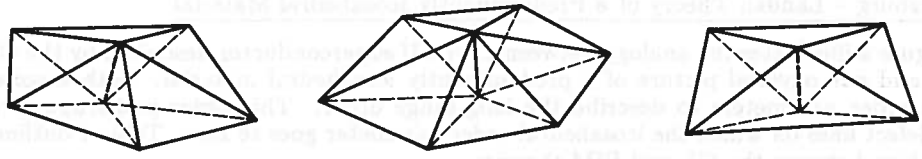

Figure 2. The three types of nearest neighbor bonds; 0°, -72° (extra tetrahedron inserted around the bond) and +72° (missing tetrahedron) disclinations [after ref. 18].

The picture of a predominantly icosahedral material is now complete. The icosahedral order parameter Q_{12} gives a quantitative measure the degree of local icosahedral ordering in the material. Regions of strong icosahedral ordering are broken up by disclination lines, which link atoms that are not in icosahedral environments. In the next section we shall develop a theory for the thermodynamic properties of a predominantly icosahedral material.

3. Thermodynamics of the Predominantly Icosahedral Material

To model the physics of a predominantly icosahedral material (PIM) we shall draw upon an analogy with the Ginzburg-Landau theory of type II superconductors. Once this analogy has been established, the PIM theory will be seen to have many non-linearities which make it nearly impossible to attack analytically. A numerical study of the model is performed by discretizing the theory using the well established techniques of lattice gauge theory.

3.1 Ginzburg – Landau Theory of Superconductivity

In the Ginzburg-Landau (GL) theory of superconductivity, the order parameter is the complex scalar electron condensate wave function ψ. The external field which interacts with the condensate is the magnetic field $\vec{H}$. The free energy functional for a superconductor is [30],

$$F = \frac{1}{2m^*} \mid (-i\hbar\nabla - \frac{e^*}{c}\vec{A})\psi \mid^2 + \alpha \mid \psi \mid^2 + \frac{\mid \vec{H} \mid^2}{8\pi} + \gamma \mid \psi \mid^3 + \frac{1}{2}\beta \mid \psi \mid^4 + \ldots, \quad (1)$$

where m^* and e^* are the effective mass and charge of the electrons, $\vec{A}$ is the vector potential associated with the magnetic field $\vec{H}$, and α, β, γ are, in general, temperature dependent parameters. This energy expansion is valid near the phase transition where $\mid \psi \mid$ is small.

Superconductors are characterized by their diamagnetic properties. This is observed through the Meissner effect, i.e. the sudden exclusion (either total or partial) of magnetic

flux from the bulk of the material as it becomes superconducting. Type I materials are characterized by their perfect diamagnetism in the bulk. A type II superconductor exists in the mixed state, characterized by a partial penetration of magnetic flux into the bulk [31].

3.2 Ginzburg – Landau Theory of a Predominantly Icosahedral Material

Figure 3 illustrates the analogy between a type II superconductor described by the GL theory and our physical picture of a predominantly icosahedral material. Both theories contain order parameters to describe the long-range order. This order is disrupted by linear defect lines on which the icosahedral order parameter goes to zero. Table 1 outlines the analogy between the GL and PIM theories.

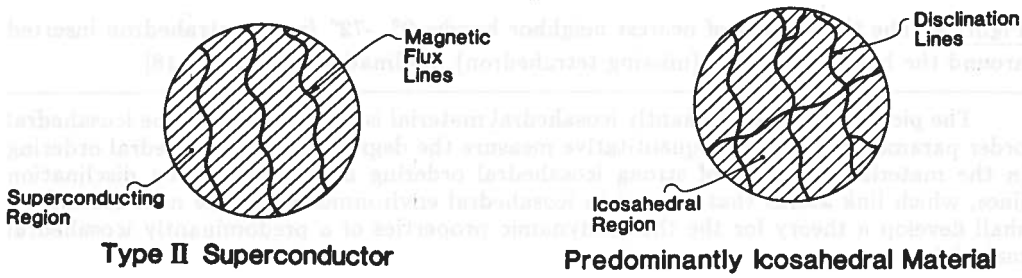

Figure 3. Comparison of the type II superconductor and a predominantly icosahedral material.

Table 1. The formal analogy between the Ginzburg-Landau theory of superconductivity and the gauge field theory of predominantly icosahedral materials (PIM).

Ginzburg-Landau	PIM
Condensate Wavefunction, ψ	Icosahedral Order Parameter, $Q_{12.m_1m_2}$
Abrikosov Flux Lattice	Disclination Line Network
Meissner Effect	Disclination Flux Exclusion

Using Table 1 as a guide, an energy expansion for the PIM can be written down in analogy with equation 1;

$$F = \frac{1}{2}\sum_{m} | D_\mu Q_{12.m} |^2 + \alpha \sum_{m} | Q_{12.m} |^2 + \frac{1}{3} | F_{\mu\nu} |^2 + \text{higher order terms} \qquad (2)$$

The first term in equation 2 is a covariant derivative,

$$D_\mu Q_{12,m} = \sum_{m'} [\delta_{m,m'}\partial_\mu - i\kappa(A_\mu)_{m,m'}]\, Q_{12,m'},$$

where κ is the coupling constant between the order parameter and disclination line fields, m represents the set $\{m_1, m_2\}$. A_μ is the potential associated with the disclination lines in analogy with the vector potential of the magnetic field. The third term in equation 2 accounts for the self-energy of the disclination line network. As with the electromagnetic contribution to the total energy of a type II superconductor, this term involves the absolute square of the tensor;

$$F_{\mu\nu} \equiv \partial_\mu A_\nu - \partial_\nu A_\mu - i\kappa[A_\mu, A_\nu].$$

In a superconductor the commutator between different components of the vector potential is zero, i.e. the magnetic field is Abelian, meaning that magnetic flux lines can be combined to produce the same resulting line irrespective of how they are brought together. In a PIM, the potential is a non-Abelian field hence the disclination lines behave in a much more complicated and non-linear manner.

The Meissner effect in a type II superconductor will have an interesting analogy in the PIM. Below a critical temperature, the disclination lines in the bulk of a PIM will be (at least partially) expelled. This exclusion of disclination line flux may permit long-range ordering to occur in the icosahedral order parameter field. Thus the Meissner effect will be analogous to a transition from a high temperature disordered PIM (or liquid) to a low temperature phase with enhanced short-range icosahedral order.

3.3 The Discretized Theory

We can investigate the equilibrium thermodynamics of a predominantly icosahedral material starting from the partition function;

$$Z = \sum_{\text{states}} e^{-\beta \int d^3x\, F(Q_{12,m}(\vec{x}),\vec{A})},$$

where the sum is over all possible configurations of the order parameter and disclination line fields. This quantity can be effectively calculated using a Monte Carlo sampling technique since only those field configurations near the equilibrium configuration will make significant contributions to the sum. To implement the Monte Carlo sampling technique, the energy expansion in equation 2 must be made discrete. This is accomplished by using the techniques of lattice gauge theory.

In recent years, lattice gauge theories have been developed as a means of studying the complicated non-linear properties of the quark-gluon plasma [32]. In this approach one uses a discrete space-time approximation, with the matter field placed on the lattice sites of a 4-dimensional hypercubic lattice and the gauge field transporters on the links between the sites. One then writes down a discretized energy functional in terms of the lattice site and link variables. The partition function and any thermodynamic quantities and order parameters can then be calculated approximately by means of Monte Carlo sampling.

The discrete version of the PIM theory can be constructed in direct analogy with lattice gauge theory. A discrete cubic lattice is introduced with the icosahedral order parameter (Q_{12}) on the lattice sites and the disclination line potential (A) on the links between the sites. Next, a discretized version of equation 2 is written in terms of the lattice site and link variables.

The covariant derivative term of equation 2 can be easily expressed as the difference between the order parameter at site j and the order parameter at site i transported back to j (under the influence of the neighboring disclination lines). A simple form for this is;

$$| D_\mu Q_{12,m}(\vec{x}_j) |^2 \longrightarrow \frac{1}{a^2} \sum_{i \text{ n.n. } j} | Q_{12,m}(\vec{x}_j) - U_{ji} Q_{12,m}(\vec{x}_i) |^2,$$

where a is the lattice parameter and the sum is taken over the nearest neighbors i of site j. The quantity $U_{ji} \equiv e^{iA(\frac{x_i+x_j}{2})a}$ is called a transporter because multiplication by this quantity represents the effect of the disclination lines on the order parameter as it is moved from x_i to x_j.

Following Wilson [33], the third term in equation 2 can be written as a sum over plaquettes (i.e. elementary squares of links in the lattice) of a function of disclination field transporter products;

$$| F_{\mu\nu} |^2 \longrightarrow \sum_{\text{plaquettes } \square} (1 - \text{Re Tr}(U_\square)),$$

where $U_\square$ is the product of transporters around an elementary square of the lattice, and the trace can be taken in one of several matrix representations of the transporters.

The discretized energy expansion finally becomes;

$$F = \sum_{\substack{i \text{ n.n. } j \\ m}} | Q_{12,m}(\vec{x}_j) - U_{ji} Q_{12,m}(\vec{x}_i) |^2 + \alpha \sum_m | Q_{12,m} |^2 + \frac{1}{3} \sum_{\text{plaquettes } \square} f(U_\square) + \text{higher order terms}, \tag{3}$$

where $f(U_\square)$ is a function which determines the energy associated with the disclination lines (see Table 2).

3.4 Phase Structure of the Predominantly Icosahedral Material

A Monte Carlo sampling of all the possible configurations of the order parameter and frustration fields in a calculation of the partition function would be astronomically time consuming. In order to reduce the number of available states, and the computational labor, we are compelled to reduce the number of degrees of freedom available to the site and link variables. These simplifications are physically motivated.

As noted in section 2.3, all of the defect lines present in topologically close-packed intermetallic compounds are simple $-72°$ disclinations (i.e. one tetrahedron has been added to a nearest neighbor bond). Analysis of the Bernal holes in metallic glasses show that in addition to the $-72°$ disclinations, there are mainly $+72°$ disclination lines present [18]. With these observations in mind, we can restrict the number of possible defect lines to just the 0° (i.e. no disclination) and $\pm 72°$ disclination lines. The spectrum of energies per unit length that we have chosen for the disclinations is given in Table 2. We wish to favor the presence of 0° disclination lines since they are found in icosahedral coordinations. Hence the energy of a 0° disclination line is established as zero. The energy per unit length of a Kasper (-72°) disclination line is parameterized by E_l. The value of E_l will be

determined after comparing the results of this theory with experiment. Since the Bernal (+72°) disclination line is found in metastable metallic glass structures, it is given a slightly higher energy per unit length.

Table 2. Values of the energy per unit length of all disclination lines used in the Monte Carlo simulations of a predominantly icosahedral material.

Disclination Line	Energy per Unit Length (units of E_l)
0°	0
−72° (Kasper)	1
+72° (Bernal)	1.1

As a consequence of considering only disclination line defects, we can make an important simplification to the order parameter field. Since disclinations are defect lines labelled in the form $(l,l) \in Y' \times Y'$ (where Y' is the double group of the icosahedron) [25], they can only rotate the order parameter into a limited number of new states. Because of this restriction, we shall reduce the manifold of the order parameter to be just the group Y'.

The numerical model of a predominantly icosahedral material is now complete. On the lattice sites is an icosahedral order parameter field which can take on values given by elements of the discrete double group of the icosahedron Y'. Between the sites there exist disorder field transporters whose plaquette products U_σ are also elements of the group Y'. We have used a Monte Carlo sampling algorithm to study the phase structure of this model material.

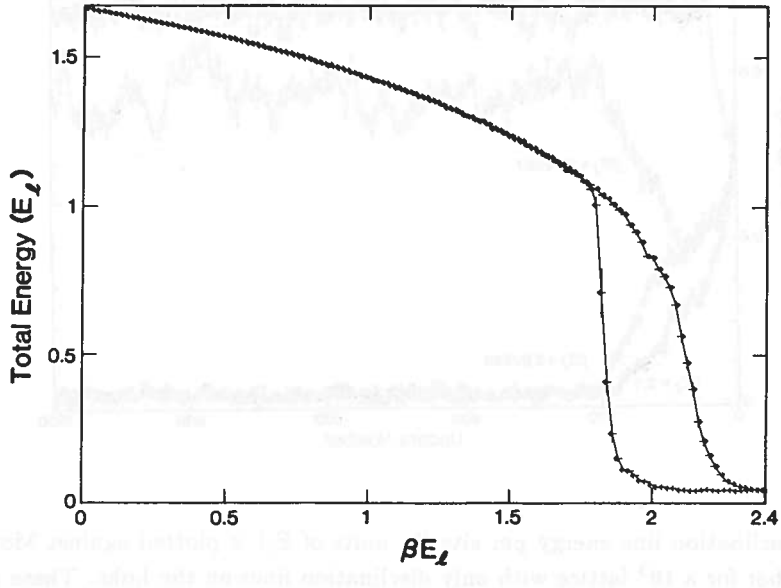

Figure 4. Cyclic annealing treatment of a 16^3 lattice with only disclination lines present. The energy per site of the disclination lines (in units of E_l) is plotted against the dimensionless inverse temperature $E_l/k_B T$.

3.5 Results

In this paper, we shall consider only the simplest version of the PIM model. Consider a PIM in which we ignore the icosahedral order parameter, Q_{12} and retain just the disclination lines discussed above. This model describes the density of icosahedral short-range order in the PIM and does not address the possibility of long-range correlations in the orientation of icosahedral regions. This simple model already displays some interesting and non-trivial behavior. In what follows, we shall examine a PIM consisting of interacting disclination lines and described by just the third term in equation 3.

Figure 4 shows a cyclic annealing run between βE_l ($\equiv E_l/k_B T$) = 0 to 2.4 and back to 0. The energy per site (in units of E_l) is due to just the disclination lines (i.e. the third term in both equations 2 and 3). In this version of the model, the disclination lines alone produce the observed first order transition around $\beta E_l \simeq 2$. The transition was isolated by starting the system in a mixed initial configuration. A half block of the lattice links were set to the identity element (i.e. no disclinations are present through the plaquettes) and the links in the other half block were assigned randomly. The system is then annealed for a long period of time until the entire lattice settles into one of the two competing states. Such annealing treatments have been used to place limits on the transition temperature, $2.02397 < (\beta E_l)_c < 2.02398$ (see Figure 5).

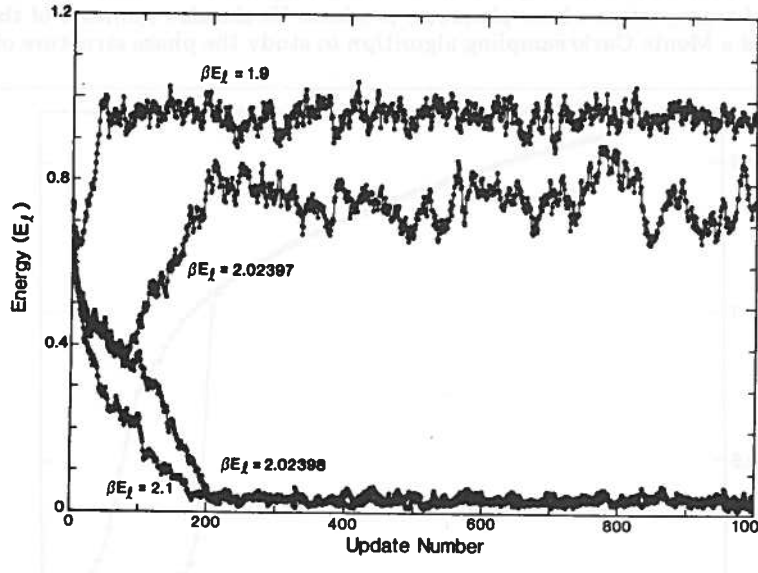

Figure 5. Disclination line energy per site (in units of E_l) is plotted against Monte Carlo update number for a 16^3 lattice with only disclination lines on the links. These annealing treatments are carried out both above and below the transition temperature.

The high temperature phase is characterized by a high density of disclination line defects. This high density of defects implies that many of the atomic sites are not icosahedral symmetry sites. This high temperature phase may then represent a liquid or cubo-octahedral crystalline solid. On the other hand, the low temperature phase has very few disclination lines, implying that most of the atoms sit in icosahedral environments. The model predicts a phase transition from a high temperature (icosahedrally) disordered phase to a low temperature phase with high icosahedral site symmetry.

4. Comparison of Theory and Experiment

4.1 Fixing Theoretical Parameters

By comparing the results of annealing treatments on the model predominantly icosahedral material (PIM) with experimental results for icosahedral phase formation, we can fix the parameter E_l. The first order phase transition observed in the PIM model is qualitatively similar to the formation of the icosahedral phase from a rapidly quenched liquid metal. Anlage et al. [34] have estimated that the peritectic formation temperature of icosahedral Al-Ru is about 1500K. Using the calculated value of $(\beta E_l)_c$ we find that $E_l \simeq \frac{1}{4}$ eV/nearest neighbor bond length is the energy per unit length of a Kasper disclination line in Al-Ru.

The latent heat of the freezing transition can be estimated from Figures 4 and 5. One finds that $\Delta H_c \simeq 1.0 E_l$ (since $\Delta(PV) = 0$). With the above value of E_l, the latent heat amounts to about 0.25 eV/site in Al-Ru. Richard's rule [35] says that the latent heat per site for a typical metal is about 0.2 eV/site. This overestimate of the latent heat is due to the small number of disclination lines (hence low entropy) of the low temperature phase. A physical material must contain a non-zero density of disclination lines. Such a material will have a higher entropy and smaller heat of formation than the PIM model low temperature phase.

4.2 Summary and Conclusions

A long-range ordered icosahedral phase has been observed in samples of certain rapidly quenched liquid metals. In an attempt to explain this observation, we propose a model predominantly icosahedral material (PIM). This PIM is endowed with short-range icosahedral order just like that believed to exist in supercooled liquid metals. By physical arguments, we find that the $\pm 72°$ disclinations are the most interesting defects in such a material.

By analogy with the well known gauge theories of physics (in particular the Ginzburg-Landau theory of superconductivity), we propose a free energy functional to describe the PIM. Once the theory is constructed, it is then straightforward to investigate the equilibrium thermodynamic properties of the system by means of a modified Monte Carlo lattice gauge theory analysis. The results of a simplified version of the theory are compared to the liquid $\rightarrow$ icosahedral phase freezing transition. The energy per unit length of a Kasper disclination in Al-Ru is found to be approximately $\frac{1}{4}$ eV/nearest neighbor bond length.

The author wishes to acknowledge discussions with W. L. Johnson, E. J. Cotts, B. Fultz, R. B. Schwarz, and P. D. Askenazy as well as financial support from the Eastman Kodak and I.B.M. corporations.

REFERENCES

1) Hamermesh, M.: Group Theory and its Application to Physical Problems, (Addison-Wesley, Reading, Mass., 1962), p.51.
2) Kittel, C.: Introduction to Solid State Physics, (J. Wiley, New York, 1976), p. 9.
3) Burns, G.: Solid State Physics, (Academic Press, Orlando, 1985), p. 46.
4) Zallen, R.: The Physics of Amorphous Solids, (Wiley, New York, 1983), p. 58.
5) Pauling, L.: The Nature of the Chemical Bond, 3rd ed. (Cornell University Press, Ithaca, 1960).
6) Frank, F. C.: Proc. Roy. Soc. (London), Ser. A, 1952, 215, 43.
7) Hoare, M. R. and Pal, P.: Adv. Phys., 1971, 20, 161.
8) Hoare, M.: Ann. N.Y. Acad. Sci., 1976, 279, 186.
9) Turnbull, D.: J. Metals, Trans. A.I.M.E., 1950, 188, 1144.
10) Perepezko J. H. and Paik, J. S.: J. Non-Cryst. Solids, 1984, 61&62, 113.
11) Samson, S.: Structural Chemistry and Molecular Biology, ed. by A. Rich (W. H. Freeman, San Francisco, 1968), p. 687.
12) Samson, S.: in Developments in the Structural Chemistry of Alloy Phases, ed. by B. C. Giessen (Plenum, New York, 1969), p. 65.
13) Walford, L. K.: Acta Cryst., 1964, 17, 57.
14) Bergman, G., Waugh, J. L. T. and Pauling, L.: Acta Cryst., 1957, 10, 254.
15) Bernal, J. D.: in Liquids : Structure, Properties, Solid Interactions, ed. by T. J. Hughel (Elsevier, Amsterdam, 1965), p. 25.
16) Steinhardt, P. J., Nelson, D. R. and Ronchetti, M.: Phys. Rev. Lett., 1981, 47, 1297.
17) Steinhardt, P. J., Nelson, D. R. and Ronchetti, M.: Phys. Rev. B, 1983, 28, 784.
18) Nelson, D. R.: Phys. Rev. Lett., 1983, 50, 982 ; Phys. Rev. B, 1983, 28, 5515.
19) Kléman, M. and Sadoc, J. F.: J. Phys. Lett. (Paris), 1979, 40, L-569.
20) Sadoc, J. F.: J. Non-Cryst. Solids, 1981, 44, 1.
21) Sachdev, S. and Nelson, D. R.: Phys. Rev. Lett., 1984, 53, 1947.
22) Sachdev, S. and Nelson, D. R.: Phys. Rev. B, 1985, 32, 1480.
23) Toulouse, G.: Commun. Phys., 1977, 2, 115.
24) Schechtman, D., Blech, I., Gratias, D. and Cahn, J. W.: Phys. Rev. Lett., 1984, 53, 1951.
25) Nelson, D. R. and Widom, M.: Nucl. Phys. B, 1984, 240, 113.
26) Coxeter, H. S. M.: Regular Polytopes, (Dover, New York, 1973).
27) Sinha, A. K.: Prog. Mat. Sci., 1972, 15, 79.
28) Frank, F. C. and Kasper, J. S.: Acta Cryst., 1958, 11, 184.
29) Frank, F. C. and Kasper, J. S.: Acta Cryst., 1959, 12, 483.
30) Tinkham, M.: Introduction to Superconductivity, (McGraw-Hill, New York, 1975), p. 104.
31) Rose-Innes, A. C. and Rhoderick, E. H.: Introduction to Superconductivity, (Pergamon, Oxford, 1978), p. 183.
32) Rebbi, C.: Lattice Gauge Theories and Monte Carlo Simulations, (World Scientific, Singapore, 1983).
33) Wilson, K.: Phys. Rev. D, 1974, 10, 2445.
34) Anlage, S. M., Fultz, B., and Krishnan, K.: submitted to J. Mater. Res., 1987.
35) Swalin, R. A.: Thermodynamics of Solids, (Wiley, New York, 1962), p. 59.